

SEISMIC DESIGN LOAD DISTRIBUTION IN STEEL FRAME

Y. Deguchi¹, T. Kawashima¹, M. Yamanari² and K. Ogawa³

¹ Graduate Student, Graduate School of Science and Technology, Kumamoto University, Kumamoto, Japan

² Associate Professor, Graduate School of Science and Technology, Kumamoto University, Kumamoto, Japan

³ Professor, Graduate School of Science and Technology, Kumamoto University, Kumamoto, Japan

Email: ogawa@kumamoto-u.ac.jp, yamanari@kumamoto-u.ac.jp

ABSTRACT:

In this paper, we present the seismic design load distribution. First, the equation of the distribution of seismic load in the design is presented. It is based on the assumption that the velocity spectrum of ground motion is independent of the natural period, and it is deduced from the maximum shear response of the elastic shear bar with both uniform stiffness and mass distributions. Then, two equations were selected from the equations with respect to the seismic design load distributions that have already been proposed in Japan. A comparison of these equations was carried out with regard to both leveling of the story drift angle distribution and minimization of the maximum story drift angle in all the stories of a multistory frame.

KEYWORDS: Earthquake-Resistant Design, Story Shear Coefficient, Maximum Story Drift

1. INTRODUCTION

When multistory frame structures with a relatively weak story are subjected to severe earthquakes, the seismic deformation concentrates at the story, resulting in structural collapse. Recent earthquake-resistant designs face serious problems that make story deformation and damage uniform over the height of the structure.

In the current seismic code of Japan [BCJ 1997], the story strength is indicated by the yield shear force Q_{yi} , described as

$$Q_{yi} = C_i W_i = C_i \alpha_i W_T \quad (1.1)$$

where W_T is the total weight of the structure, W_i is the weight above the story, and α_i is the value in which W_i is divided by W_T . C_i is called the yield shear coefficient: it specifies the intensity and vertical distribution of the seismic load.

$$C_i = C_B A_i \quad (1.2)$$

Here, C_B is called the base shear coefficient; it is the shear coefficient of the bottom story. A_i is the shear coefficient distribution (A_i distribution); it represents the vertical distribution of the seismic load. In this sense, many previous researches have analyzed the A_i distribution from various viewpoints.

In this paper, the equation of the distribution of the seismic load in the design was obtained based on a simple theoretical analysis. Then, two equations were selected from the equations obtained with respect to the distribution of the seismic loads that have already been proposed in Japan. A comparison between these equations was carried out.

2. SHEAR COEFFICIENT DISTRIBUTION

Researches investigating the distribution of the maximum shear force of a story in an elastic system and the optimum shear coefficient distribution in an elastoplastic system along the height in order to develop uniform plastic deformations for each story have already been conducted [Kobori et al. 1970] [Kato et al. 1977]. They

are summarized as follows.

1. The shear coefficient distribution is plotted for a narrow range irrespective of the number of stories, stiffness distribution, and mass distribution, in case that the shear coefficient is expressed as a function of α_i in which the weight above the story is divided by the total weight of the structure.
2. The shear coefficient distribution, which was determined to make the damage distribution of a frame uniform, almost coincides with the story distribution of the maximum shear coefficient of an elastic structure, except for at the top story.

The current seismic code of Japan is based on above-mentioned results. It is shown that the shear coefficient distribution for a story is a function of a value α_i and the story shear coefficient distribution required in elastic design is the same that required in plastic design.

It seems rational that the distribution of the design shear coefficient can be archived through a suite of numerical works using model-shear-type multi-lumped mass systems with sufficient degrees of freedom so as to obtain it as a function of α_i . In this sense, the seismic response analysis would have been performed on 20 or fewer mass types [Kato et al. 1977]. However, if an earthquake response analysis using a shear-type model with as many degrees of freedom can be obtained, then this procedure is more suitable with regard to a shear-type stick model (shear bar) with infinite number of mass. Further, according to the results obtained from researches involving similar conditions to the ones mentioned above, if the distribution of the design shear coefficient—expressed as a function of α_i —is not influenced by the stiffness and mass distributions, it is simplistic; further, an elastic solid in which the mass is thoroughly distributed can be employed.

Therefore, the maximum shear response is deduced by means of an elastic shear bar with both uniform stiffness and mass distributions. In this study, the maximum shear response obtained by means of an elastic shear bar is mainly assumed to be an object; therefore, the intensity of the maximum shear response does not pose a problem. This implies that the maximum shear response can be investigated by means of the elastic structure because of the consideration that the shape of the load distribution of the elastic structure is similar to an elastoplastic structure.

Consider an elastic shear bar of length H , as shown Fig. 2.1, is subjected to ground motion \ddot{y} . It is assumed that the elastic shear bar is uniform with shearing stiffness G and distributed mass ρ . When the damping is neglected, the equation of dynamic equilibrium can be expressed as [N. M. Newmark et al. 1972]

$$\rho \frac{\partial^2 v}{\partial t^2} - G \frac{\partial^2 v}{\partial x^2} = -\rho \ddot{y} \quad (2.1)$$

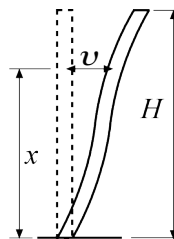


Figure 2.1 Elastic shear bar

where vectors x and v denote the coordinates along the height and displacement, respectively.

In this analysis, we assume free vibration conditions, where the external force term—the right side of the above expression—is neglected. When solving this under the boundary condition, the natural circular frequency ω_k , natural period T_k , and natural mode of vibration $f_k(x)$ can be expressed as follows:

$$\omega_k = \frac{\pi(2k-1)}{2H} \sqrt{\frac{G}{\rho}} \quad (2.2)$$

$$T_k = \frac{2\pi}{\omega_k} = \frac{4H}{(2k-1)} \sqrt{\frac{\rho}{G}} \quad (2.3)$$

$$f_k(x) = \sin \frac{\pi(2k-1)x}{2H} \quad (2.4)$$

The displacement $v(t,x)$ is shown as the sum of each mode of vibration.

$$v(t,x) = \sum_{k=1}^{\infty} a_k(x) f_k(x) \quad (2.5)$$

By substituting Eqn. 2.5 into Eqn. 2.1, we obtain the normal modes of vibration that are orthogonal. Further, by considering viscous damping, it can be shown that the motion of the system can be described by the following equation for the k -th mode of vibration:

$$\ddot{a}_k(t) + 2\zeta_k \omega_k \dot{a}_k(t) + \omega_k^2 a_k(t) = -\beta_k \ddot{y} \quad (2.6)$$

where ζ_k and β_k denote the damping ratio and participation factor in the k -th mode of vibration and β_k is expressed as

$$\beta_k = \frac{\int_0^H \rho f_k(x) dx}{\int_0^H \rho f_k(x) f_k(x) dx} = \frac{8}{\pi(2k-1)} \quad (2.7)$$

where if the simulated velocity response spectrum of \ddot{y} is expressed as a function $S_V(T)$ with period T , the maximum response $a_{k,\max}$ of $a_k(t)$ can be described by the following equation:

$$a_{k,\max} = \frac{\beta_k}{\omega_k} S_V(T_k) = \frac{16H}{\pi^2(2k-1)^2} \sqrt{\frac{\rho}{G}} S_V(T_k) \quad (2.8)$$

The shear force $Q(t,x)$ used for analytical purposes is described by the following equation:

$$Q(t,x) = \sum_{k=1}^{\infty} a_k(t) G \frac{df_k(x)}{dx} \quad (2.9)$$

The maximum shear force $Q_{\max}(x)$ can be expressed as the square root of the sum of the squares to obtain the maximum response.

$$Q_{\max}(x) = \sqrt{\sum_{k=1}^{\infty} \left\{ a_{k,\max} G \frac{df_k(x)}{dx} \right\}^2} = \frac{8\sqrt{\rho G}}{\pi} \sqrt{\sum_{k=1}^{\infty} \frac{S_V^2(T_k)}{(2k-1)^2} \cos^2 \frac{\pi(2k-1)x}{2H}} \quad (2.10)$$

It is assumed that the velocity response spectrum of ground motion is independent of the natural period.

$$S_V(T) = S_{VO}(\text{constant}) \quad (2.11)$$

Therefore, Eqn. 2.10 becomes

$$\begin{aligned}
 Q_{\max}(x) &= \frac{8\sqrt{\rho G} S_{VO}}{\pi} \sqrt{\sum_{k=1}^{\infty} \frac{1}{(2k-1)^2} \cos^2 \frac{\pi(2k-1)x}{2H}} \\
 &= \frac{8\sqrt{\rho G} S_{VO}}{\pi} \sqrt{\sum_{k=1}^{\infty} \frac{1}{(2k-1)^2} \frac{1 + \cos \frac{\pi(2k-1)x}{H}}{2}} \\
 &= S_{VO} \sqrt{8\rho G \frac{H-x}{H}}
 \end{aligned} \tag{2.12}$$

The above equation can be resolved by using the following series formulae:

$$\begin{aligned}
 \sum_{k=1}^{\infty} \frac{1}{(2k-1)^2} &= \frac{\pi^2}{8} \\
 \sum_{k=1}^{\infty} \frac{1}{(2k-1)^2} \cos \frac{\pi(2k-1)y}{c} &= \frac{\pi^2 \left(\frac{c}{2} - y \right)}{4c}, \quad 0 < y < c
 \end{aligned}$$

The shear coefficient is obtained from the maximum shear force $Q_{\max}(x)$ (Eqn. 2.12) divided by the weight above this point $g\rho(H-x)$ (g denotes the acceleration due to gravity). Further, the shear coefficient distribution A_i is obtained by division with the base shear coefficient as follows.

$$A_i = \frac{Q_{\max}(x)}{g\rho(H-x)} / \frac{Q_{\max}(0)}{g\rho H} = 1 / \sqrt{\frac{H-x}{H}} \tag{2.13}$$

Here, the dimensionless height α_i is

$$\alpha_i = \frac{\int_x^H g\rho dx}{\int_0^H g\rho dx} = \frac{H-x}{H} \tag{2.14}$$

Eqn. 2.13 can be written as

$$A_i = 1 / \sqrt{\alpha_i} \tag{2.15}$$

Eqn. 2.15 represents the distribution of the maximum shear force response of a story in an elastic structure. In a frame in which the distribution of the yield strength of each story corresponds to Eqn. 2.15, the possibility of all the stories yielding at the same time can be expected. This can be attributed to the assumption that the velocity response spectrum of the ground motion is independent of the period. Eqn. 2.15 tends to exaggerate the influence of a higher-mode response because the velocity response spectrum of ground motion has a characteristic of decreasing in proportion to the period in a short range of frequencies.

3. ANALYSIS OF SHEAR COEFFICIENT DISTRIBUTION

The proposed equation concerning A_i can be used as an object of comparison as follows.

- (1) The current seismic code of Japan [BCJ 1997] has the provision for the following equation that considers the dependence of the shear coefficient distribution A_i on the fundamental natural period of vibration T_1 .

$$A_i = 1 + \left(\frac{1}{\sqrt{\alpha_i}} - \alpha_i \right) \frac{2T_1}{1 + 3T_1} \quad (3.1)$$

where $T_1 = 0.03H$, H = height of the structure

- (2) The optimum shear coefficient distribution A_i in order to develop uniform cumulative plastic deformation at each story was obtained through a trial-and-error dynamic response analysis [Kato et al. 1982].

$$A_i = 1 + 1.5927\xi_i - 11.8519\xi_i^2 + 42.5833\xi_i^3 - 59.4827\xi_i^4 + 30.1586\xi_i^5 \quad (3.2)$$

where $\xi_i = 1 - \alpha_i$

- (3) The shear coefficient distribution A_i for this study is

$$A_i = 1 / \sqrt{\alpha_i} \quad (3.3)$$

A comparison between these equations is carried out in Figure 3.1. There is a difference in the top story of approximately 0.2 or less, and the shear coefficient distribution obtained from Eqn. 3.3 tends to yield a large value. However, this is almost coincident, except for that around the top story. Although, for a 12-story system, Eqn. 3.1 yields slightly larger values; for an 8-story system, Eqn. 3.1 and Eqn. 3.3 are equivalent; and for a 4-story system, Eqn. 3.3 yields a slightly larger value. That is the reason why the A_i distribution obtained from Eqn. 3.1 exhibits larger values near the bottom of the structure's center, although the A_i distribution of Eqn. 3.3 tends to yield slightly larger values near the top story.

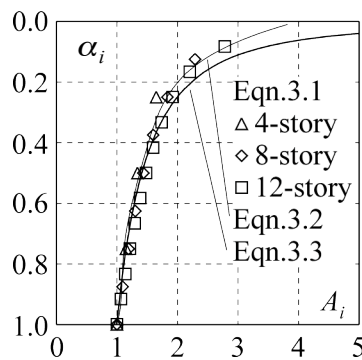


Figure 3.1 Comparison of story shear coefficient of the story for Eqn. 3.1, Eqn. 3.2, and Eqn. 3.3

3.1. Analysis Variables

The analysis is carried out for shear-type multi-lumped mass systems shown in Table 3.1. These are 4-, 8-, and 12-story systems. These systems have the same height and weight for each story. The load–deformation relation for each story under monotonic loading is expressed by a bilinear relation, and the rigidity in the inelastic behavior is adjusted to 0, 1/3, and 2/3. The structural properties are determined using standard design procedures stipulated in the seismic code of Japan [BCJ 1997]. The standard shear force coefficient C_0 and yield story drift angle R_y are listed in Table 3.1. The story drift angle reaches R_y (1/200, 1/400) against the designed earthquake force profile with a standard shear force coefficient C_0 of 0.2. The shear coefficient distribution A_i employs the three proposed equations described in the previous section, and they have been applied later to the name of the analytical systems.

Figure 3.2 shows the correlation of the fundamental natural period T_1 of each system and the sum of the design shear force for all the stories. In the abscissa, p indicates the sum of the designed shear force Q_y of the story

Table 3.1 Systems adopted in the analysis

The name of Systems	Number of stories	C_0	R_y	Rigidity in the inelastic behavior	Fundamental natural period		
					Eqn. 3.1	Eqn. 3.2	Eqn. 3.3
F12k0d2	12	0.3	0.00750	0	1.715	1.759	1.737
F12k0d4			0.00375		1.213	1.243	1.228
F12k1d2		0.2	0.00250	1/3	1.715	1.759	1.737
F12k1d4			0.00500		1.213	1.243	1.228
F12k2d2			0.00250	2/3	1.715	1.759	1.737
F12k2d4			0.00500		1.213	1.243	1.228
F8k0d2	8	0.3	0.00750	0	1.275	1.294	1.278
F8k0d4			0.00375		0.902	0.915	0.904
F8k1d2		0.2	0.00250	1/3	1.275	1.294	1.278
F8k1d4			0.00500		0.902	0.915	0.904
F8k2d2			0.00250	2/3	1.275	1.294	1.278
F8k2d4			0.00500		0.902	0.915	0.904
F4k0d2	4	0.3	0.00750	0	0.948	0.943	0.931
F4k0d4			0.00375		0.670	0.667	0.658
F4k1d2		0.2	0.00250	1/3	0.948	0.943	0.931
F4k1d4			0.00500		0.670	0.667	0.658
F4k2d2			0.00250	2/3	0.948	0.943	0.931
F4k2d4			0.00500		0.670	0.667	0.658

for each system according to the three A_i distributions as the comparison object that were normalized with the sum of all the Q_y values of the systems set by using A_i from Eqn. 3.3.

The difference in the fundamental natural period T_1 by the A_i distribution set is small (Figure 3.2). A decreasing trend can be recognized in T_1 ; that is, as the strength increases, the rigidity increases. The p values are in the range of 0.96 to 1.02; that is, the strength is almost equal to the system employing the A_i distribution.

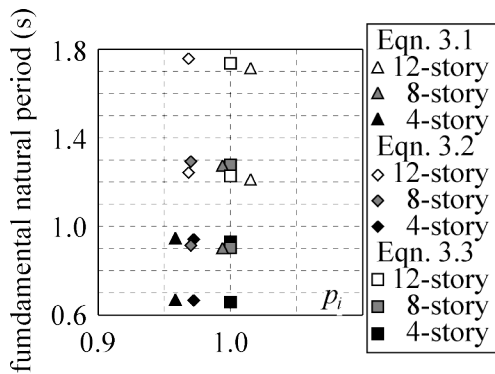


Figure 3.2 Comparison of fundamental natural period T_1 .

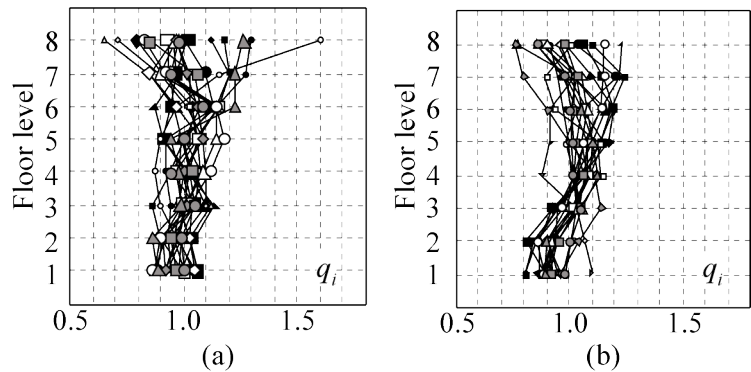


Figure 3.3 Story distribution of the maximum story shear force of the system (F08k1d2): (a) 10/50; (b) 2/50

3.2. Dynamic Response Analysis

Suites of ground motions used in the FEMA/SAC project [Somerville P, et al. 1997] were used for the dynamic response analysis of the systems. Here, 2 sets of 20 records were used that represent the probabilities of exceedance to be 10% and 2% in 50 years in the Los Angeles area (USA), denoted as the 10/50 and 2/50 record sets, respectively. For the first two modes, Rayleigh damping of 2% was adopted in the analysis. The P-Δ effect was not included in the analysis.

Figure 3.3 shows the results when the system (F08k1d2) was subjected to all of the 40 ground motions in each of the 10/50 and 2/50 record sets as the example of the results. It shows the story distribution of the maximum story shear force $Q_{max,i}$, normalized by the designed shear force for each story $Q_{y,i}$. Here, the intention is adjusted so as to make the overturning moment constant; the sum of the shear forces for each story finally becomes constant because the story height is fixed.

$$q_i = \frac{\frac{Q_{max,i}}{\sum_{i=1}^N Q_{max,i}}}{\frac{Q_{y,i}}{\sum_{i=1}^N Q_{y,i}}} \quad (3.5)$$

In Figure 3.3, the story distribution of the maximum shear force for each story fluctuates at every ground motion, and it fluctuates more significantly at the top story. This tendency is recognized in all of the systems (Table 3.1).

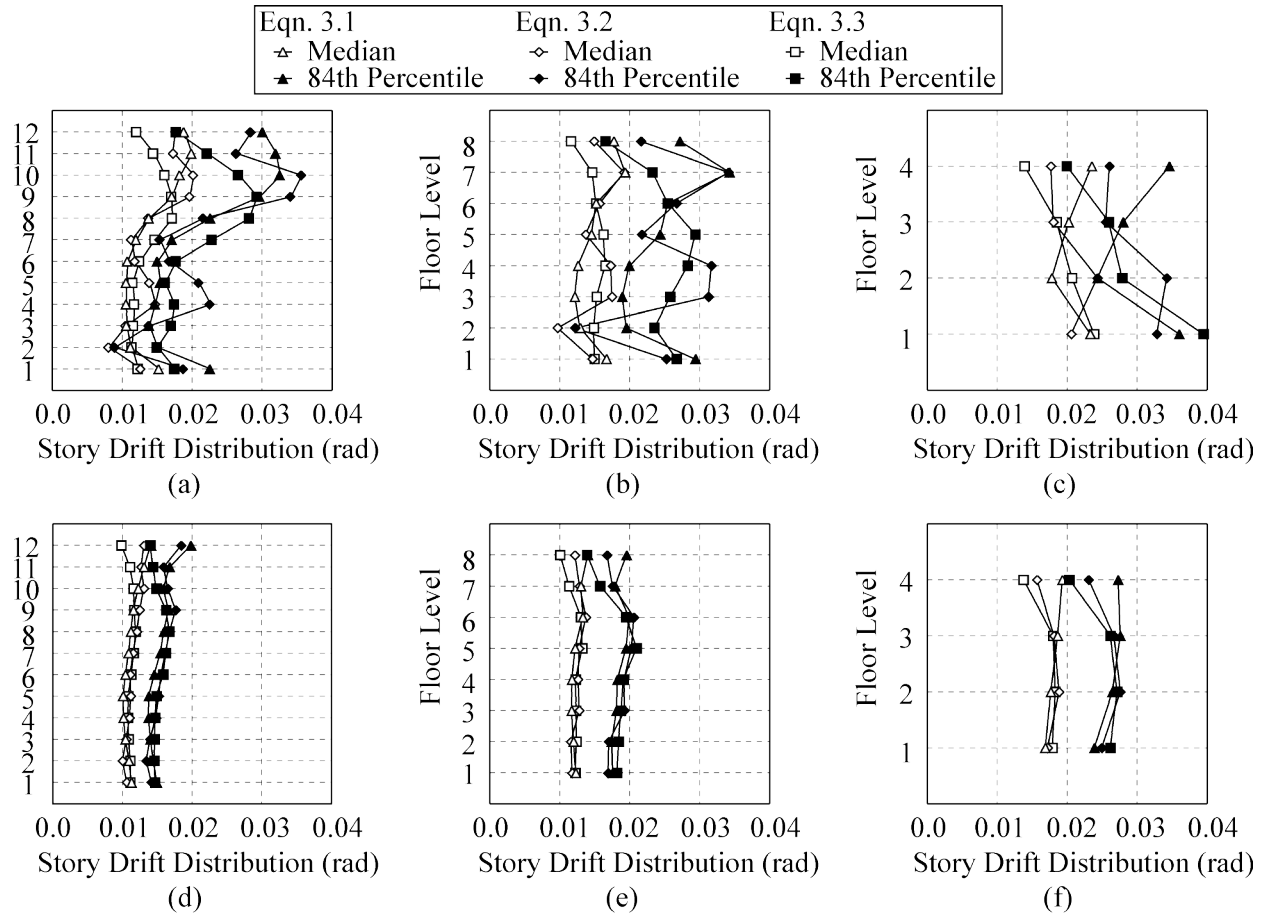


Figure 3.4 Comparison of the maximum story drift angles (10/50 median and 84th percentile responses):

(a) F12k0d2 system; (b) F08k0d2 system; (c) F04k0d2 system;

(d) F12k1d2 system; (e) F08k1d2 system; (f) F04k1d2 system

Figure 3.4 shows the distributions of the maximum story drift angles of the system with the 10/50 record set expressed as their medians and 84th percentiles. Here, the median refers to the exponent of the mean of the natural logarithmic values of the data, and 84th percentile represents the median multiplied by the exponent of the standard deviation of the natural logarithmic values of the data. The standard deviation is referred to as the dispersion and is approximately equal to the coefficient of variation.

The distribution of the maximum story drift angles is relatively uniform and close to unity for the systems in which the rigidity is 1/3 (inelastic behavior), regardless of the A_i distribution. It suggests that these three equations of the A_i distribution approximate the optimum shear coefficient distribution. Although the difference in the A_i distribution set is not large, near the top story, the distribution of the maximum story drift angles is larger for the system that employs Eqn. 3.1 and the distribution of the maximum story drift angles is smaller for the system that employs Eqn. 3.3 (Figure 3.1).

Table 3.2 shows the largest of the maximum story drift angles R_{max} occurring in the corresponding story for all the systems described in Table 3.1. Further, in comparison to R_{max} on the system set in the A_i distribution

using the three equations as a comparison object, the minimum field is shown in gray. In Table 3.2, although the difference by the A_i distribution set is not large, R_{max} for the system that employs Eqn. 3.3 is the smallest in most sections. In particular, for the systems in which the rigidity is 0 (inelastic behavior) and the systems with several stories, the difference by the A_i distribution set increases, and R_{max} for the system employing Eqn. 3.3 tends to become the smallest. Further, it is not evident that R_{max} for the system that employs Eqn. 3.1 expressing A_i as a function of the fundamental natural period tends to become the smallest.

Table 3.2 Comparison of the largest of the maximum story drift angles R_{max}

The name of Systems	Largest of maximum story drift angles $R_{max}(\times 10^{-2})$					
	10/50			2/50		
	Eqn. 3.1	Eqn. 3.2	Eqn. 3.3	Eqn. 3.1	Eqn. 3.2	Eqn. 3.3
F12k0d2	2.00	2.03	1.72	6.58	5.63	5.16
F12k0d4	1.82	1.32	1.20	7.46	6.43	5.95
F12k1d2	1.41	1.31	1.19	2.72	2.80	2.68
F12k1d4	0.83	0.86	0.87	2.21	2.24	2.20
F12k2d2	1.55	1.46	1.29	3.25	3.33	3.06
F12k2d4	1.00	0.99	0.94	2.09	2.23	2.16
F8k0d2	1.93	1.92	1.65	7.03	5.82	5.73
F8k0d4	1.79	1.57	1.56	6.09	5.54	5.67
F8k1d2	1.41	1.38	1.32	3.17	3.21	3.19
F8k1d4	0.93	0.97	0.95	2.14	2.26	2.20
F8k2d2	1.69	1.54	1.41	3.32	3.32	3.23
F8k2d4	1.02	1.02	1.00	1.90	1.96	1.95
F4k0d2	2.35	2.43	2.38	7.06	6.43	7.14
F4k0d4	2.17	1.99	2.22	7.52	7.25	7.52
F4k1d2	1.93	1.89	1.83	4.50	4.32	4.21
F4k1d4	1.30	1.28	1.26	2.97	3.00	2.92
F4k2d2	2.16	1.93	1.91	3.91	3.77	3.71
F4k2d4	1.32	1.23	1.21	2.76	2.79	2.71

4. CONCLUSIONS

1. An equation for the seismic load distribution, $A_i = 1/\sqrt{\alpha_i}$, was obtained based on the assumption that the velocity spectrum of the ground motion is independent of the period. Further, it is obtained from the maximum shear response using the elastic shear bar with both uniform stiffness and mass distributions.
2. It was clarified that the equation $A_i = 1/\sqrt{\alpha_i}$ is the most effective and useful, because it yields the least value of the largest of the maximum story drift angles R_{max} occurring in the corresponding story; moreover, it has the simplest equation.

REFERENCES

- Building Center of Japan (1997). BCJ Seismic provisions for design of building structures. The Building Center of Japan, Tokyo (in Japanese).
- Kobori, T. and Minai, R. (1970). On the Optimum Aseismic Design Data for Multi-Story Structures Based on Elasto-Plastic Earthquake Response. *Proc. of the 3rd European Symposium on Earthquake Engineering*, 435-445
- Kato, B. and Akiyama, H. (1977). Earthquake resistant design for steel buildings. *Proc. of the 6th WCEE* 2, 1945-1950
- N. M. Newmark and E. Rosenblueth. (1972). Fundamentals of Earthquake Engineering, Prentice Hall, 305-319
- Kato, B. and Akiyama, H. (1982). Seismic design of steel buildings. *Journal of the Structural Division* 108:ST8, 1709-1721
- Somerville P, et al. (1997). Development of ground motion time histories for phase 2 of the FEMA=SAC steel project, SAC Background Document, Report No. SAC=BD-97-04, SAC Joint Venture, 555 University Ave., Sacramento, CA.